

A Series of Cu^{II}-Azide Polymers of Cu₆ Building Units and the Role of Chelating Diamine in Controlling their Dimensionality: Synthesis, Structures, and Magnetic Behavior

Sandip Mukherjee and Partha Sarathi Mukherjee*

Department of Inorganic and Physical Chemistry, Indian Institute of Science, Bangalore-560012, India

Received August 20, 2010

Four new neutral copper-azido polymers [Cu₆(N₃)₁₂(aem)₂]_n (**1**), [Cu₆(N₃)₁₂(dmeen)₂(H₂O)₂]_n (**2**), [Cu₆(N₃)₁₂(N,N'-dmen)₂]_n (**3**), and [Cu₆(N₃)₁₂(hmpz)₂]_n (**4**) [aem = 4-(2-aminoethyl)morpholine; dmeen = N,N-dimethyl-N'-ethylethylenediamine; N,N'-dmen = N,N'-dimethylethylenediamine and hmpz = homopiperazine] have been synthesized by using 0.33 mol equiv of the chelating diamine ligands with Cu(NO₃)₂·3H₂O/CuCl₂·2H₂O and an excess of NaN₃. Single crystal X-ray structures show that the basic unit of these complexes, especially **1–3**, contains very similar Cu^{II}₆ building blocks. But the overall structures of these complexes vary widely in dimensionality. While **1** is three-dimensional (3D) in nature, **2** and **3** have a two-dimensional (2D) arrangement (with different connectivity) and **4** has a one-dimensional (1D) structure. Cryomagnetic susceptibility measurements over a wide range of temperature exhibit dominant ferromagnetic behavior in all the four complexes. The experimental susceptibility data have been analyzed by some theoretical model equations.

Introduction

The field of polynuclear coordination assemblies has been an area of intense study over the past decade, not only for their interesting molecular topologies but also for the fact that they may be designed with specific functionalities.¹ Using paramagnetic metal centers to form clusters or extended networks has also proved very rewarding for the understanding of the fundamental magnetic phenomena, such as long-range ordering, spin canting, metamagnetism, anisotropy, relaxation dynamics, and quantum tunneling of magnetization, both experimentally and theoretically.²

Designed and serendipitous assembly, the two main approaches to these materials, use contrasting synthetic protocols. The designed assemblies can be structurally controlled and hence exhibit tunable chemical and physical properties.

However, directed synthesis is still a great challenge because the assembly progress is highly influenced by several factors, such as the metal/ligand nature, solvents, templates, and counterions.³ Recently, the concept of secondary building units (SBUs) has been applied with eminent success to the design of metal organic frameworks (MOFs).⁴ Such SBUs can be connected into MOFs by appropriate bridging ligands. In serendipitous assembly, novel structural topologies can be achieved (which are otherwise difficult to predesign) by using one or several bridging ligands and coligands in a variety of combinations. The versatility shown by the azido ligand (N₃[−]) in its bridging modes (Scheme 1), along with its ability to couple paramagnetic metal centers ferromagnetically under

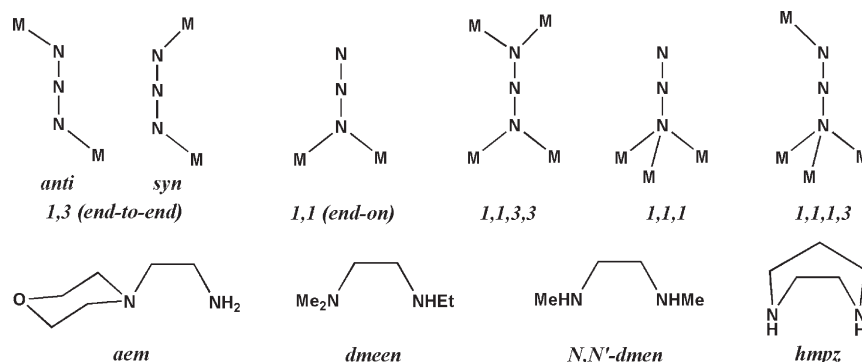
*To whom correspondence should be addressed. Fax: 91-80-23601552; tel: 91-80-22933352; e-mail: psm@ipc.iisc.ernet.in.

(1) (a) Stamatatos, T. C.; Christou, A. G.; Jones, C. M.; O'Callaghan, B. J.; Abboud, K. A.; O'Brien, T. A.; Christou, G. *J. Am. Chem. Soc.* **2007**, *129*, 9840. (b) Bagai, R.; Abboud, K. A.; Christou, G. *Inorg. Chem.* **2007**, *46*, 5567. (c) Vittal, J. J. *Coord. Chem. Rev.* **2007**, *251*, 1781. (d) Yoon, J.; Solomon, E. I. *Coord. Chem. Rev.* **2007**, *251*, 379. (e) Lee, C. F.; Leigh, D. A.; Pritchard, R. G.; Schults, D.; Teat, S. J.; Timco, G. A.; Wimpenny, R. E. P. *Nature* **2009**, *458*, 314. (f) Wimpenny, R. E. P. *Angew. Chem. Int. Ed.* **2008**, *47*, 7992. (g) Wimpenny, R. E. P. *Dalton Trans.* **2002**, 1. (h) Chandrasekhar, V.; Murugesapandian, B. *Acc. Chem. Res.* **2009**, *42*, 1047. (i) Chandrasekhar, V.; Murugesapandian, B.; Vittal, J. J.; Clérac, R. *Inorg. Chem.* **2009**, *48*, 1148.

(2) (a) Gatteschi, D.; Sessoli, R. *Angew. Chem.* **2003**, *115*, 278. Gatteschi, D.; Sessoli, R. *Angew. Chem., Int. Ed.* **2003**, *42*, 268; (b) Aromí, G.; Brechin, E. K. *Struct. Bonding (Berlin)* **2006**, *122*, 1. (c) Coulon, C.; Miyasaka, H.; Clérac, R. *Struct. Bonding (Berlin)* **2006**, *122*, 163.

(3) (a) Banfi, S.; Carlucci, L.; Caruso, E.; Ciani, G.; Proserpio, D. M. *Dalton Trans.* **2002**, 2714. (b) Gable, R. W.; Hoskins, B. F.; Robson, R. *Chem. Commun.* **1990**, 1677. (c) Subramanian, S.; Zaworotko, M. J. *Angew. Chem., Int. Ed.* **1995**, *34*, 2127. (d) Long, D.-L.; Blake, A. J.; Champness, N. R.; Wilson, C.; Schroder, M. *Chem.—Eur. J.* **2002**, *8*, 2027. (e) Hennigar, T. L.; MacQuarrie, D. C.; Losier, P.; Rogers, R. D.; Zaworotko, M. J. *Angew. Chem., Int. Ed.* **1997**, *36*, 972. (f) Tong, M.-L.; Ye, B.-H.; Chen, X.-M.; Ng, S. W. *Inorg. Chem.* **1998**, *37*, 2645. (g) Gudbjartson, H.; Biradha, K.; Poirier, K. M.; Zaworotko, M. J. *J. Am. Chem. Soc.* **1999**, *121*, 2599. (h) Su, C.-Y.; Cai, Y.-P.; Chen, C.-L.; Lissner, F.; Kang, B.-S.; Kaim, W. *Angew. Chem., Int. Ed.* **2002**, *41*, 3371. (i) Carlucci, L.; Ciani, G.; Proserpio, D. M. *Angew. Chem., Int. Ed.* **1995**, *34*, 1895. (j) Bino, A.; Shweky, I.; Cohen, S.; Bauminger, E. R.; Lippad, S. J. *Inorg. Chem.* **1998**, *37*, 5168. (k) Blake, A. J.; Champness, N. R.; Hubberstey, P.; Li, W.-S.; Withersby, M. A.; Schroder, M. *Coord. Chem. Rev.* **1999**, *183*, 117. (l) Zhu, H.-L.; Tong, Y.-X.; Chen, X.-M. *J. Chem. Soc., Dalton Trans.* **2000**, 4182.

(4) (a) Millward, A. R.; Yaghi, O. M. *J. Am. Chem. Soc.* **2005**, *127*, 17998. (b) Rosi, N. L.; Kim, J.; Eddaoudi, M.; Chen, B.; O'Keeffe, M.; Yaghi, O. M. *J. Am. Chem. Soc.* **2005**, *127*, 1504. (c) Ockwig, N. W.; Delgado-Friedrichs, O.; O'Keeffe, M.; Yaghi, O. M. *Acc. Chem. Res.* **2005**, *38*, 176.

Scheme 1. Common Bridging Modes of the Azido Ligand (top) and the Diamine Ligands Used in the Present Study (bottom)

suitable conditions, makes it a very popular choice in serendipitous assembly.^{5–11}

High-dimensional metal-azido systems are of particular interest, due to the possibility of enhancement of the bulk magnetic properties. In the neutral Cu-azido systems with chelating diamine ligands, the dimensionalities are determined by the relative molar quantities of copper and the diamine ligand.¹¹ Higher equivalents of the chelating ligand reduces the available sites on the metal for coordination by the bridging azido ligand and thus generally leads to lower dimensional structures. A simple change in the substitution

on the diamine ligand can also dramatically change the structure and magnetic behavior of the metal-azido systems.¹¹ Variation in the amount of blocking diamine ligand should in principle change the structural pattern of Cu-azido systems. A strategy to have more coordination sites available around the metal center for a short bridging ligand such as azide may bring several metal ions closer and favor the formation of cluster as building unit. For this purpose, use of lower equivalents of blocking amine is expected to be fruitful. This prompted us to see the effect of the amount (less than one equivalent) of the blocking diamine as well as the nature of diamine on the overall structure and magnetic behavior. Here we report the synthesis, structural characterization, and variable temperature magnetic behavior of four new Cu-azido coordination polymers $[\text{Cu}_6(\text{N}_3)_{12}(\text{aem})_2]_n$ (**1**), $[\text{Cu}_6(\text{N}_3)_{12}(\text{dmeen})_2(\text{H}_2\text{O})_2]_n$ (**2**), $[\text{Cu}_6(\text{N}_3)_{12}(\text{N},\text{N}'\text{-dmen})_2]_n$ (**3**), and $[\text{Cu}_6(\text{N}_3)_{12}(\text{hmpz})_2]_n$ (**4**), [aem = 4-(2-aminoethyl)morpholine;

(5) (a) Papaefstathiou, G. S.; Perlepes, S. P.; Escuer, A.; Vicente, R.; Font-Bardia, M.; Solans, X. *Angew. Chem., Int. Ed.* **2001**, *40*, 884. (b) Papaefstathiou, G. S.; Escuer, A.; Vicente, R.; Font-Bardia, M.; Solans, X.; Perlepes, S. P. *Chem. Commun.* **2001**, 2414. (c) Boudalis, A. K.; Donnadieu, B.; Nastopoulos, V.; Clemente-Juan, J. M.; Mari, A.; Sanakis, Y.; Tuchagues, J.-P.; Perlepes, S. P. *Angew. Chem., Int. Ed.* **2004**, *43*, 2266. (d) Nanda, P. K.; Aromi, G.; Ray, D. *Inorg. Chem.* **2006**, *45*, 3143. (e) Mandal, D.; Bertolasi, V.; Ribas-Ariño, J.; Ray, D. *Inorg. Chem.* **2008**, *47*, 3465. (f) Mukherjee, P.; Drew, M. G. B.; Gómez-García, C. J.; Ghosh, A. *Inorg. Chem.* **2009**, *48*, 5848. (g) Chattopadhyay, S.; Drew, M. G. B.; Diaz, C.; Ghosh, A. *Dalton Trans.* **2007**, 2492.

(6) (a) Naiya, S.; Biswas, C.; Drew, M. G. B.; Gómez-García, C. J.; Clemente-Juan, J. M.; Ghosh, A. *Inorg. Chem.* **2010**, *49*, 6616. (b) Biswas, C.; Drew, M. G. B.; Ruiz, E.; Estrader, M.; Diaz, C.; Ghosh, A. *Dalton Trans.* **2010**, 39, 7474.

(7) (a) Ribas, J.; Escuer, A.; Monfort, M.; Vicente, R.; Cortes, R.; Lezama, L.; Rojo, T. *Coord. Chem. Rev.* **1999**, *193–195*, 1027 and references therein. (b) Kahn, O. *Chem. Phys. Lett.* **1997**, *265*, 165. (c) Aubin, S. M. J.; Bolcar, M. A.; Christou, G.; Eppley, H. J.; Foltling, K.; Hendrickson, D. N.; Huffman, J. C.; Squire, R. C.; Tsai, H.-L.; Wang, S.; Wemple, M. W. *Polyhedron* **1998**, *17*, 3005. (d) Thomas, L.; Lionti, F.; Ballou, R.; Gatteschi, D.; Sessoli, R.; Barbara, B. *Nature* **1996**, *383*, 145. (e) *Magnetic Molecular Materials*; Gatteschi, D., Kahn, O., Miller, J. S., Palacio, F., Eds.; Kluwer Academic: Dordrecht, The Netherlands, 1991. (f) Sessoli, R.; Tsai, H.-L.; Schake, A. R.; Wang, S.; Vincent, J. B.; Foltling, K.; Gatteschi, D.; Christou, G.; Hendrickson, D. N. *J. Am. Chem. Soc.* **1993**, *115*, 1804. (g) Ouellette, W.; Galán-Mascaros, J. R.; Dunbar, K. R.; Jubieta, J. *Inorg. Chem.* **2006**, *45*, 1909. (h) Shatruck, M.; Dragulescu-Andrasi, A.; Chambers, K. E.; Stoian, S. A.; Bominaar, E. L.; Achim, C.; Dunbar, K. R. *J. Am. Chem. Soc.* **2007**, *129*, 6104. (i) Tolis, E. I.; Helliwell, M.; Langley, S.; Raftery, J.; Wimpenny, R. E. P. *Angew. Chem., Int. Ed.* **2003**, *42*, 3804. (j) Ribas, J.; Escuer, A.; Monfort, M.; Vicente, R.; Cortés, R.; Lezama, L.; Rojo, T. *Coord. Chem. Rev.* **1999**, *193–195*, 1027 and references therein. (k) Kato, M.; Muto, Y. *Coord. Chem. Rev.* **1988**, *92*, 45. (l) Maji, T. K.; Mukherjee, P. S.; Mostafa, G.; Mallah, T.; Cano-Boquera, J.; Chaudhuri, N. R. *Chem. Commun.* **2001**, 1012.

(8) (a) Mondal, K. C.; Song, Y.; Mukherjee, P. S. *Inorg. Chem.* **2007**, *46*, 9736. (b) Price, D. J.; Batten, S. R.; Moubaraki, B.; Murray, K. S. *Chem. Commun.* **2002**, 762. (c) Konar, S.; Zangrando, E.; Drew, M. G. B.; Mallah, T.; Ray Chaudhuri, N. *Inorg. Chem.* **2003**, *42*, 5966. (d) Sessoli, R.; Gatteschi, D.; Caneschi, A.; Novak, M. A. *Nature* **1993**, *365*, 141. (e) Wernsdorfer, W.; Aliaga-Alcalde, N.; Hendrickson, D. N.; Christou, G. *Nature* **2002**, *416*, 406. (f) Müller, A.; Meyer, J.; Krickemeyer, E.; Beugholt, C.; Bögge, H.; Peters, F.; Schmidtman, M.; Kögerler, P.; Koop, M. J. *Chem.—Eur. J.* **1998**, *4*, 1000. (g) Leibeling, G.; Demeshko, S.; Bauer-Siebenlist, B.; Meyer, F.; Pritzkow, H. *Eur. J. Inorg. Chem.* **2004**, 2413. (h) Demeshko, S.; Leibeling, G.; Dechert, S.; Meyer, F. *Dalton Trans.* **2006**, 3458.

(9) (a) Mukherjee, P. S.; Maji, T. K.; Mostafa, G.; Mallah, T.; Ray Chaudhuri, N. *Inorg. Chem.* **2000**, *39*, 5147. (b) Comarmond, J.; Plumere, P.; Lehn, J. M.; Agnus, Y.; Louis, R.; Weiss, R.; Kahn, O.; Morgesten-Badarau, I. *J. Am. Chem. Soc.* **1982**, *104*, 6330. (c) Kahn, O.; Sikorav, S.; Gouteron, J.; Jeannin, S.; Jeannin, Y. *Inorg. Chem.* **1983**, *22*, 2877. (d) Tandon, S. S.; Thompson, L. K.; Manuel, M. E.; Bridson, J. N. *Inorg. Chem.* **1994**, *33*, 5555. (e) Ribas, J.; Monfort, M.; Ghosh, B. K.; Solans, X.; Font-Bardia, M. *J. Chem. Soc., Chem. Commun.* **1995**, 2375. (f) Ribas, J.; Monfort, M.; Ghosh, B. K.; Solans, X. *Angew. Chem., Int. Ed. Engl.* **1994**, *33*, 2087. (g) Viau, G.; Lombardi, G. M.; De Munno, G.; Julve, M.; Lloret, F.; Faus, J.; Caneschi, A.; Clemente-Juan, J. M. *Chem. Commun.* **1997**, 1195. (h) Escuer, A.; Vicente, R.; Ribas, J.; El Fallah, M. S.; Solans, X.; Font-Bardia, M. *Inorg. Chem.* **1993**, *32*, 3727. (i) Ruiz, E.; Cano, J.; Alvarez, S.; Alemany, P. *J. Am. Chem. Soc.* **1998**, *120*, 11122. (j) Shen, Z.; Zuo, J.-L.; Gao, S.; Song, Y.; Che, C.-M.; Fun, H.-K.; You, X.-Z. *Angew. Chem., Int. Ed.* **2000**, *39*, 3633. (k) Hong, C. S.; Koo, J.; Son, S.-K.; Lee, Y. S.; Kim, Y.-S.; Do, Y. *Chem.—Eur. J.* **2001**, *7*, 4243.

(10) (a) Escuer, A.; Harding, C. J.; Dussart, Y.; Nelson, J.; McKee, V.; Vicente, R. *J. Chem. Soc., Dalton Trans.* **1999**, 223. (b) Escuer, A.; Font-Bardia, M.; Massoud, S. S.; Mautner, F. A.; Penalba, E.; Solans, X.; Vicente, R. *New J. Chem.* **2004**, *28*, 681. (c) Hong, C. S.; Do, Y. *Angew. Chem., Int. Ed.* **1999**, *38*, 193. (d) Mukherjee, P. S.; Dalai, S.; Zangrando, E.; Lloret, F.; Chaudhuri, N. R. *Chem. Commun.* **2001**, 1444. (e) Saha, S.; Koner, S.; Tuchagues, J.-P.; Boudalis, A. K.; Okamoto, K.-I.; Banerjee, S.; Mal, D. *Inorg. Chem.* **2005**, *44*, 6379. (f) Thompson, L. K.; Tandon, S. S.; Manuel, M. E. *Inorg. Chem.* **1995**, *34*, 2356. (g) Mautner, F. A.; Hanna, S.; Cortés, R.; Lezama, L.; Barandika, M. G.; Rojo, T. *Inorg. Chem.* **1999**, *38*, 4647. (h) Goher, M. A. S.; Cano, J.; Journaux, Y.; Abu-Youssef, M. A. M.; Mautner, F. A.; Escuer, A.; Vicente, R. *Chem.—Eur. J.* **2000**, *6*, 778.

(11) (a) Gu, Z.-G.; Zuo, J.-L.; You, X.-Z. *Dalton Trans.* **2007**, 4067. (b) Abu-Youssef, M. A. M.; Escuer, A.; Mautner, F. A.; Ohnstrom, L. *Dalton Trans.* **2008**, 3553. (c) Gu, Z.-G.; Xu, Y.-F.; Yin, X.-J.; Zhou, X.-H.; Zuo, J.-L.; You, X.-Z. *Dalton Trans.* **2008**, 5593. (d) Mondal, K. C.; Mukherjee, P. S. *Inorg. Chem.* **2008**, *47*, 4215. (e) Jia, Q.-X.; Bonnet, M.-L.; Gao, E.-Q.; Robert, V. *Eur. J. Inorg. Chem.* **2009**, 3008. (f) Mukherjee, S.; Gole, B.; Chakrabarty, R.; Mukherjee, P. S. *Inorg. Chem.* **2009**, *48*, 11325. (g) Tian, C.-B.; Li, Z.-H.; Lin, J.-D.; Wu, S.-T.; Du, S.-W.; Lin, P. *Eur. J. Inorg. Chem.* **2010**, 427. (h) Sengupta, O.; Gole, B.; Mukherjee, S.; Mukherjee, P. S. *Dalton Trans.* **2010**, 39, 7451.

dmeen = *N,N*-dimethyl-*N'*-ethylethylenediamine; *N,N'*-dmen = *N,N'*-dimethylethylenediamine and hmpz = homopiperazine]. Among these, the first three complexes have almost identical Cu^{II}_6 core structures, but, while **1** has an overall 3D structure, the other two are 2D in nature. Interestingly, the two-dimensional (2D) arrangement of the basic unit of **2** and **3** are very much different. However, complex **4**, though having the same ratio of copper and diamine, has a very dissimilar hexanuclear building block that extends in one dimension. All the four complexes were found to be dominantly ferromagnetic in nature.

Experimental Section

Materials. $\text{Cu}(\text{NO}_3)_2 \cdot 3\text{H}_2\text{O}$, $\text{CuCl}_2 \cdot 2\text{H}_2\text{O}$, NaN_3 , 4-(2-aminoethyl)morpholine, *N,N*-dimethyl-*N'*-ethylethylenediamine (dmeen), *N,N'*-dimethylethylenediamine (*N,N'*-dmen), and homopiperazine (hmpz) were obtained from commercial sources and were used as received without further purification.

Physical Measurements. Elemental analyses of C, H, and N were performed using a Perkin-Elmer 240C elemental analyzer. IR spectra were recorded as KBr pellets using a Magna 750 FT-IR spectrophotometer. The measurements of variable-temperature magnetic susceptibility were carried out on a Quantum Design MPMS-XL5 SQUID magnetometer. Susceptibility data were collected using an external magnetic field of 0.2 T for all the complexes in the temperature range of 1.8–300 K. The experimental susceptibility data were corrected for diamagnetism (Pascal's tables).¹²

Caution! Although we did not experience any problems with the compounds reported in this work, azido complexes of metal ions in the presence of organic ligands are potentially explosive. Only a small amount of material should be prepared, and it should be handled with care.

Synthesis of Complex $[\text{Cu}_6(\text{N}_3)_{12}(\text{aem})_2]_n$ (1**).** To a 10 mL methanolic solution of $\text{CuCl}_2 \cdot 2\text{H}_2\text{O}$ (1.00 mmol, 170 mg) and aem (0.33 mmol, 43 mg) an aqueous solution of NaN_3 (10.00 mmol, 650 mg) dissolved in 2 mL of water was added slowly. The mixture was stirred for 15 min and filtered. Rectangular black crystals of **1** were obtained in 48 h. Isolated yield: 35%. Anal. Calcd for **1**, $\text{C}_{12}\text{H}_{28}\text{N}_{40}\text{O}_2\text{Cu}_6$: C, 12.58; H, 2.46; N, 48.89. Found: C, 12.65; H, 2.52; N, 48.80. IR (KBr, cm^{-1}): 2026, 2060 and 2094(vs) for the azido groups.

Synthesis of the Complex $[\text{Cu}_6(\text{N}_3)_{12}(\text{dmeen})_2(\text{H}_2\text{O})_2]_n$ (2**).** To a 10 mL methanolic solution of $\text{Cu}(\text{NO}_3)_2 \cdot 3\text{H}_2\text{O}$ (1.00 mmol, 242 mg) and dmeen (0.33 mmol, 38 mg) an aqueous solution of NaN_3 (10.00 mmol; 650 mg) dissolved in 2 mL of water was added slowly. The mixture was stirred for 5 min and filtered. Rod-shaped black crystals of **2** were obtained in 24 h. Isolated Yield: 50%. Anal. Calcd for **2**, $\text{C}_{12}\text{H}_{36}\text{N}_{40}\text{O}_2\text{Cu}_6$: C, 12.49; H, 3.14; N, 48.55. Found: C, 12.33; H, 3.20; N, 48.89. IR (KBr, cm^{-1}): 2029, 2058 and 2084(vs) for the azido groups.

Synthesis of the Complex $[\text{Cu}_6(\text{N}_3)_{12}(\text{N,N}'\text{-dmen})_2]_n$ (3**).** To a 10 mL methanolic solution of $\text{CuCl}_2 \cdot 2\text{H}_2\text{O}$ (1.00 mmol, 170 mg) and *N,N'*-dmen (0.33 mmol, 29 mg) an aqueous solution of NaN_3 (10.00 mmol; 650 mg) dissolved in 2 mL of water was added slowly. The mixture was stirred for 15 min and filtered. Prismatic black crystals of **3** were obtained in 24 h. Isolated Yield: 32%. Anal. Calcd for **3**, $\text{C}_8\text{H}_{24}\text{N}_{40}\text{Cu}_6$: C, 9.05; H, 2.78; N, 52.76. Found: C, 9.12; H, 2.86; N, 52.42. IR (KBr, cm^{-1}): 2021, 2050, and 2080 for the azido groups.

Synthesis of the Complex $[\text{Cu}_6(\text{N}_3)_{12}(\text{hmpz})_2]_n$ (4**).** To a 10 mL methanolic solution of $\text{Cu}(\text{NO}_3)_2 \cdot 3\text{H}_2\text{O}$ (1.00 mmol, 242 mg) and hmpz (0.33 mmol, 33 mg) an aqueous solution of NaN_3

(10.00 mmol; 650 mg) dissolved in 2 mL of water was added slowly. The mixture was stirred and heated at 50 °C for 15 min and filtered hot. Rod-shaped black crystals of **4** were obtained in 10 h. Isolated Yield: 58%. Anal. Calcd for **4**, $\text{C}_{10}\text{H}_{24}\text{N}_{40}\text{Cu}_6$: C, 11.06; H, 2.23; N, 51.60. Found: C, 11.30; H, 2.41; N, 51.93. IR (KBr, cm^{-1}): 2030, 2061, and 2079 for the azido groups.

X-ray Crystallographic Data Collection and Refinements. Single crystal X-ray data for **1–4** were collected on a Bruker SMART APEX CCD diffractometer using the SMART/SAINT software.¹³ Intensity data were collected using graphite-monochromatized Mo-K α radiation (0.71073 Å) at 293 K. The structures were solved by direct methods using the SHELX-97¹⁴ program incorporated into WinGX.¹⁵ Empirical absorption corrections were applied with SADABS.¹⁶ All non-hydrogen atoms were refined with anisotropic displacement coefficients. The hydrogen atoms bonded to carbon and nitrogen were included in geometric positions and given thermal parameters equivalent to 1.2 times those of the atom to which they were attached. The hydrogen atoms of the coordinated water molecule in **2** could not be located. Structures were drawn using ORTEP-3 for Windows.¹⁷ Crystallographic data and refinement parameters are given in Table 1, and important interatomic distances and angles are given in Tables 2 (for **1–3**) and 3 (for **4**).

Results and Discussion

Synthesis. All the four complexes were obtained from the reactions of $\text{Cu}(\text{NO}_3)_2 \cdot 3\text{H}_2\text{O}$ or $\text{CuCl}_2 \cdot 2\text{H}_2\text{O}$ and 0.33 mol equiv of chelating diamine ligands with an excess of NaN_3 in a MeOH/ H_2O mixture. Using an excess of NaN_3 normally ensures the prevention of the immediate precipitation, allowing the crystallization of multidimensional compounds via self-assembly of the smaller units. Although **1–3** were synthesized under room temperature, for **4** heating of the reaction mixture was essential. Though the crystallization processes are simple, the choice of the Cu^{II} salts seems to be vital; in the juxtaposed experiments when we tried to synthesize the complexes with other common Cu^{II} salts (NO_3^- , SO_4^{2-} , AcO^- , Cl^- , ClO_4^-) than those reported here, we were not able to crystallize these complexes. It would thus seem to be more appropriate to call these “syntheses” as “crystallization techniques” instead.

Intense and broad multiple infrared absorptions of azido stretching vibrations in the range from 2021 to 2094 cm^{-1} are consistent with the presence of various bonding modes of the bridging azido ligands.

Structure Description of $[\text{Cu}_6(\text{N}_3)_{12}(\text{aem})_2]_n$ (1**).** The crystal structure of complex **1** consists of hexanuclear building units extended in three dimensions bridged by the azido anions (Figure 1). The asymmetric unit consists of three metal atoms, one bidentate chelating aem ligand, and six azido anions. The diamine coordinates to one of the Cu^{II} atoms (Cu1) at one end of the linear trinuclear unit and the other two metals have only azido anions in their coordination sphere. Two of these trinuclear layers

(13) SMART/SAINT; Bruker AXS, Inc.:Madison, WI, 2004.

(14) Sheldrick, G. M. *SHELX-97*; University of Göttingen: Göttingen, Germany, 1998.

(15) Farrugia, L. J. *J. Appl. Crystallogr.* **1999**, *32*, 837. Farrugia, L. J. *WinGX*, version 1.65.04; Department of Chemistry, University of Glasgow: Glasgow, Scotland, 2003.

(16) Sheldrick, G. M. *SADABS*; University of Göttingen: Göttingen, Germany, 1999.

(17) Farrugia, L. J. *ORTEP-3 for Windows*, version 1.08; *J. Appl. Crystallogr.* **1997**, *30*, 565.

(12) (a) Dutta, R. L.; Syamal, A. *Elements of Magnetochemistry*, 2nd ed.; East West Press: Manhattan Beach, CA, 1993. (b) Kahn, O. *Molecular Magnetism*; VCH Publisher: Weinheim, 1993

Table 1. Crystallographic Data and Refinement Parameters for 1–4

	1	2	3	4
empirical formula	C ₁₂ H ₂₈ N ₄₀ O ₂ Cu ₆	C ₁₂ H ₃₆ N ₄₀ O ₂ Cu ₆	C ₈ H ₂₄ N ₄₀ Cu ₆	C ₁₀ H ₂₄ N ₄₀ Cu ₆
fw	1145.90	1153.96	1061.82	1085.84
T (K)	296(2)	293 (2)	296(2)	293(2)
crystal system	monoclinic	triclinic	triclinic	monoclinic
space group	P2 ₁ /c	P $\bar{1}$	P $\bar{1}$	P2 ₁ /c
a/Å	8.5010(3)	9.6797(5)	8.4648(3)	12.526(2)
b/Å	12.9761(4)	10.2117(5)	10.5388(5)	20.654(4)
c/Å	16.8519(5)	11.0171(5)	11.3126(6)	6.9239(12)
α/deg	90.00	94.050(3)	99.827(2)	90.00
β/deg	97.538(2)	100.111(3)	102.911(2)	102.710(3)
γ/deg	90.00	111.710(3)	113.017(2)	90.00
V/Å ³	1842.87(10)	985.04(8)	867.10(7)	1747.3(5)
Z	4	2	2	4
ρ _{calcd} (g cm ⁻³)	2.065	1.939	2.034	2.064
μ (mm ⁻¹)	3.482	3.257	3.687	3.662
λ/Å	0.71073	0.71073	0.71073	0.71073
F(000)	1140	574	526	1076
collected reflns	38013	19930	9896	14968
unique reflns	5619	5634	4997	4112
GOF (F ²)	1.043	0.995	1.022	1.043
R ₁ ^a	0.0243	0.0493	0.0380	0.0379
wR ₂ ^b	0.0564	0.1085	0.0832	0.0730

$$^a R_1 = \sum ||F_o| - |F_c|| / \sum |F_o|, ^b wR_2 = \sum \{w(F_o^2 - F_c^2)^2\} / \sum \{w(F_o^2)^2\}^{1/2}.$$

Table 2. Selected Bond Distances (Å) and Angles (deg) for 1–3

1							
Cu1–N1	2.0845(13)	Cu1–N2	1.9973(15)	Cu1–N3 ^{#1}	2.5442(14)	Cu1–N5 ^{#3}	2.4607(18)
Cu1–N6	2.0213(13)	Cu1–N15	2.0388(14)	Cu2–N3	1.9916(13)	Cu2–N6 ^{#1}	2.0188(14)
Cu2–N9	2.0132(14)	Cu2–N9 ^{#1}	2.6655(13)	Cu2–N12	2.0162(14)	Cu2–N20 ^{#2}	2.4116(17)
Cu3–N3 ^{#1}	2.3938(14)	Cu3–N9	2.0235(13)	Cu3–N12	2.0299(14)	Cu3–N14 ^{#4}	2.8262(20)
Cu3–N15	2.0086(15)	Cu3–N18	1.9729(15)				
N1–Cu1–N2	85.33(6)	Cu1–N3–Cu2	93.19(6)	Cu1–N6–Cu2 ^{#1}			110.38(6)
Cu2–N9–Cu3	100.43(6)	Cu2–N12–Cu3	100.11(6)	Cu1–N3–Cu3			84.43(6)
Cu1–N15–Cu3	110.21(7)	Cu2–N9–Cu2 ^{#1}	99.63(6)				
2							
Cu1–N1	2.052(4)	Cu1–N2	2.025(3)	Cu1–N3	2.435(3)	Cu1–N6	2.058(3)
Cu1–N8 ^{#7}	2.661(4)	Cu1–N15 ^{#5}	2.011(4)	Cu2–N3	1.977(3)	Cu2–N6	2.018(3)
Cu2–N9	1.998(3)	Cu2–N9 ^{#5}	2.738(5)	Cu2–N12	1.990(3)	Cu2–O1W	2.596(4)
Cu3–N3 ^{#5}	2.567(4)	Cu3–N9	2.015(3)	Cu3–N12	2.022(3)	Cu3–N15	2.020(3)
Cu3–N18	1.980(4)	Cu3–N20 ^{#6}	2.450(4)				
N1–Cu1–N2	85.63(15)	Cu1–N3–Cu2	96.02(13)	Cu1–N6–Cu2			107.79(15)
Cu2–N9–Cu3	102.04(15)	Cu2–N12–Cu3	102.11(15)	Cu1–N3–Cu3			84.60(15)
Cu1 ^{#5} –N15–Cu3	113.32(18)	Cu2–N9–Cu2	100.34(15)				
3							
Cu1–N1	2.024(3)	Cu1–N2	2.022(2)	Cu1–N3	2.427(3)	Cu1–N6	2.016(2)
Cu1–N15 ^{#1}	2.038(2)	Cu1–N17 ^{#9}	2.576(3)	Cu2–N3	1.994(2)	Cu2–N6	1.983(3)
Cu2–N9	1.993(3)	Cu2–N9 ^{#1}	2.782(3)	Cu2–N12	2.028(2)	Cu2–N20 ^{#8}	2.470(3)
Cu3–N3 ^{#1}	2.425(3)	Cu3–N9	2.002(2)	Cu3–N12	2.022(3)	Cu3–N14 ^{#8}	2.787(4)
Cu3–N15	2.036(3)	Cu3–N18	1.946(3)				
N1–Cu1–N2	85.41(11)	Cu1–N3–Cu2	93.17(9)	Cu1–N6–Cu2			107.46(11)
Cu2–N9–Cu3	102.37(11)	Cu2–N12–Cu3	100.47(11)	Cu1–N3–Cu3 ^{#1}			85.68(8)
Cu1–N15–Cu3 ^{#1}	108.16(12)	Cu2–N9–Cu2	96.96(11)				

^{#1} –x, –y + 1, –z. ^{#2} –x – 1, –y + 1, –z. ^{#3} x, –y + 3/2, z + 1/2. ^{#4} –x – 1, –y + 1, –z. ^{#5} –x, –y, –z + 1. ^{#6} –x, –y + 1, –z + 1. ^{#7} –x, –y, –z + 2. ^{#8} –x + 1, –y + 1, –z. ^{#9} x, +y, +z + 1.

come close in space from opposite directions and are held together by 10 end-on azido bridges (six $\mu_{1,1}$ and four $\mu_{1,1,1}$) to form the Cu₆ unit, reflecting the presence of inversion center at origin, as well as the 2-fold screw axis along the crystallographic *b* axis and the glide plane perpendicular to the *b* axis. All three metal centers have distorted octahedral geometries. Cu1 has two nitrogen

atoms from the diamine ligand (N1, N2) and two other $\mu_{1,1}$ nitrogen atoms of two azido ligand (N6, N15) in its equatorial plane with the bonds in the range 1.9973(15)–2.0845(13) Å. The axial nitrogen atoms are provided by two $\mu_{1,1,1,3}$ azido [Cu1–N3, 2.5442(14) Å; Cu1–N5, 2.4607(18) Å] groups. Cu2 forms its equatorial bonds with two $\mu_{1,1}$ nitrogen atoms [Cu2–N6^{#1}, 2.0188(14) Å;

Table 3. Selected Bond Distances (Å) and Angles (deg) for 4

4							
Cu1–N1	1.990(2)	Cu1–N2	1.986(2)	Cu1–N3	1.996(3)	Cu1–N6	1.999(3)
Cu1–N20	2.474(3)	Cu2–N3	1.988(3)	Cu2–N6	1.999(3)	Cu2–N9	1.966(3)
Cu2–N12	1.996(3)	Cu2–N15 ^{#10}	2.488(3)	Cu3–N9	1.988(3)	Cu3–N12	2.035(3)
Cu3–N15	1.950(3)	Cu3–N18	1.932(3)				
N1–Cu1–N2	78.81(11)	Cu1–N3–Cu2	100.95(11)	Cu1–N6–Cu2	100.48(12)		
Cu2–N9–Cu3	102.53(13)	Cu2–N12–Cu3	99.85(13)	Cu2–N15–Cu3	103.47(12)		

^{#10} $x, -y + 1/2, z - 1/2$.

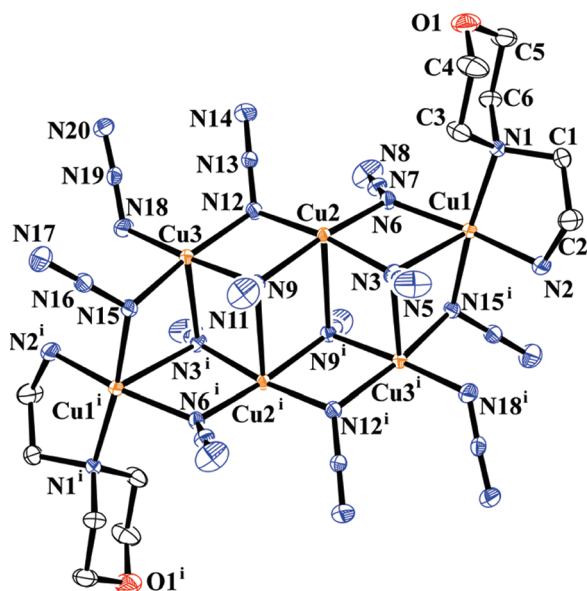


Figure 1. ORTEP view of the basic unit of **1**. Hydrogen atoms have been removed for clarity. Thermal ellipsoids are at the 30% probability level.

Cu2–N12, 2.0162(14) Å] and two $\mu_{1,1,1}$ nitrogen atoms [Cu2–N3, 1.9916(13) Å; Cu2–N9, 2.0132(14) Å] of four azido groups, whereas the axial bonds are formed by one $\mu_{1,1,1}$ nitrogen atom [Cu2–N9^{#1}, 2.6655(13) Å] and another $\mu_{1,3}$ -azido nitrogen atom [Cu2–N20^{#2}, 2.4116(17) Å] from an adjacent hexanuclear unit. The equatorial sites of Cu3 are occupied by two $\mu_{1,1}$ nitrogen atoms trans to each other (N12, N15), one $\mu_{1,1,1}$ nitrogen (N9) and one nitrogen of a $\mu_{1,3}$ azido ligand (N18) with the bonds in the range 1.9729(15)–2.0299(14) Å. The axial sites are taken up by one $\mu_{1,1,1}$ nitrogen [Cu3–N3^{#1}, 2.3938(14) Å] and one nitrogen atom from a $\mu_{1,1,3}$ azido group [Cu3–N14^{#4}, 2.8262(20) Å].

Within the basic Cu^{II}_6 core, the Cu–N($\mu_{1,1}$)–Cu angles are spread within the range 84.43(6)–110.38(6)°. The adjacent Cu–Cu distances are within the range of 3.1019(3)–3.5989(2) Å. Each Cu^{II}_6 unit is joined by two neighboring such units through double $\mu_{1,3}$ and double $\mu_{1,1,3}$ azido bridges along the *a* axis forming 1D chains (Figure 2a) and with four other units through single $\mu_{1,1,1,3}$ azido ligands to yield a complicated 3D network (Figure 2b).

Structure Description of $[\text{Cu}_6(\text{N}_3)_{12}(\text{dmeen})_2(\text{H}_2\text{O})_2]_n$ (2**).** The crystal structure of complex **2** reveals a very similar hexanuclear core structure to that of **1**, but unlike **1** it extends in two dimensions instead of three (Figure 3). The asymmetric unit consists of three crystallographically different Cu^{II} atoms, one bidentate chelating dmeen ligand (bound to Cu1), six azido anions, and one coordinated (to

Cu2) water molecule. Two of these trinuclear units come close in space from opposite directions and are held together by 10 end-on azido bridges (six $\mu_{1,1}$ and four $\mu_{1,1,1}$) to form the Cu_6 unit, while the remaining two azido groups help to extend the structure. The space group $P\bar{1}$ implies the presence of inversion center (at the origin) as the only symmetry element, which is reflected in the basic as well as the overall structure of the molecule. All the three metal atoms have distorted octahedral geometries. Cu1 has two nitrogen atoms from the diamine ligand (N1, N2) and two other $\mu_{1,1}$ nitrogen atoms of two azido ligand (N6, N15) in its equatorial plane with the bonds in the range 2.011(4)–2.058(3) Å. The two axial nitrogen atoms are provided by one $\mu_{1,1,1}$ azido [Cu1–N3, 2.435(3) Å] and one $\mu_{1,1,3}$ azido [Cu1–N8^{#7}, 2.661(4) Å] group from an adjacent Cu_6^{II} unit. Cu2 forms its equatorial bonds with two $\mu_{1,1}$ nitrogen atoms [Cu2–N6, 2.018(3) Å; Cu2–N12, 1.990(3) Å] and two $\mu_{1,1,1}$ -nitrogen atoms [Cu2–N3, 1.977(3) Å; Cu2–N9, 1.998(3) Å] of four azido groups, whereas the axial bonds are formed by one oxygen atom of a water molecule [Cu2–O1W, 2.596(4) Å] and another $\mu_{1,1,1}$ nitrogen atom [Cu2–N9^{#5}, 2.738(5) Å]. The equatorial sites of Cu3 are occupied by two $\mu_{1,1}$ nitrogen atoms trans to each other (N12, N15), one $\mu_{1,1,1}$ nitrogen (N9) and one nitrogen from a $\mu_{1,3}$ azido ligand (N18) with the bonds in the range from 1.980(4) to 2.022(3) Å. The axial sites are taken up by one $\mu_{1,1,1}$ nitrogen [Cu3–N3^{#5}, 2.567(4) Å] and one nitrogen atom from a $\mu_{1,3}$ azido group [Cu3–N20^{#6}, 2.450(4) Å] from an adjacent Cu_6 unit.

Within the basic Cu^{II}_6 core, the Cu–N($\mu_{1,1}$)–Cu angles are spread within the range 84.60(15)° to 113.32(18)°. The adjacent Cu–Cu distances are within the range of 3.1202(7)–3.6679(8) Å. Each Cu^{II}_6 unit is joined with two neighboring such units through double $\mu_{1,3}$ azido bridges, that join two Cu3 atoms along the *b* axis and with two other units through double $\mu_{1,1,3}$ azido ligands parallel to the *c* axis to yield a 2D network (Figure 4a).

Structure Description of $[\text{Cu}_6(\text{N}_3)_{12}(\text{N},\text{N}'\text{-dmeen})_2]_n$ (3**).** The crystal structure of complex **3** shows the presence of a hexanuclear core structure (Figure 5) very similar to that of **1** and **2**, which extends in two dimensions. The asymmetric unit consists of three crystallographically different Cu^{II} atoms, one bidentate chelating N,N'-dmeen ligand (bound to Cu1), and six azido anions. Two of these trinuclear units come close in space from opposite directions and are held together by 10 azido bridges (six $\mu_{1,1}$ and four $\mu_{1,1,1}$) to form the Cu_6 unit, while the remaining two azido groups help to extend the structure. The spatial arrangement of the asymmetric units by the action of the inversion center generates the basic hexanuclear structure, as well as the overall 2D network. All three metal atoms have

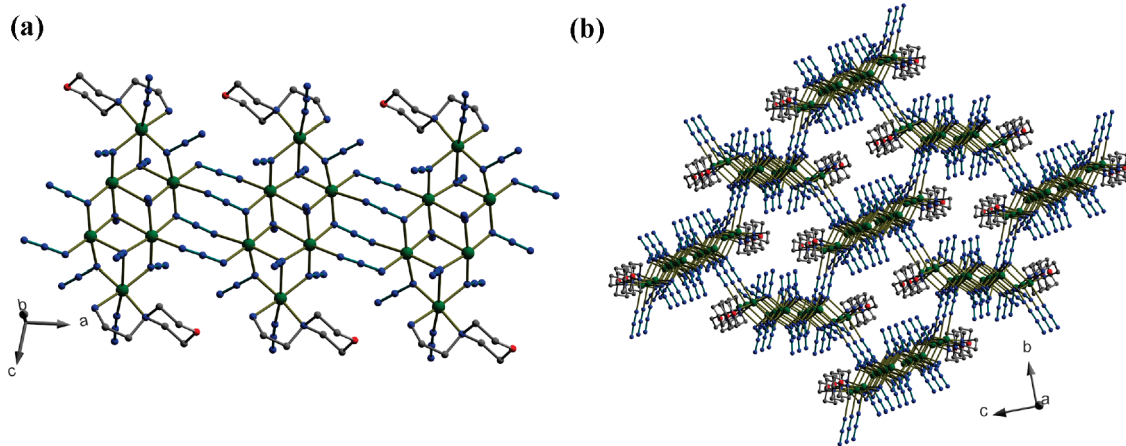


Figure 2. (a) Ball and stick view of the chains of Cu^{II}_6 units that run along the a axis and (b) the overall 3D structure of **1**. Color code: copper – green, nitrogen – blue, carbon – gray. Hydrogen atoms have been removed for sake of clarity.

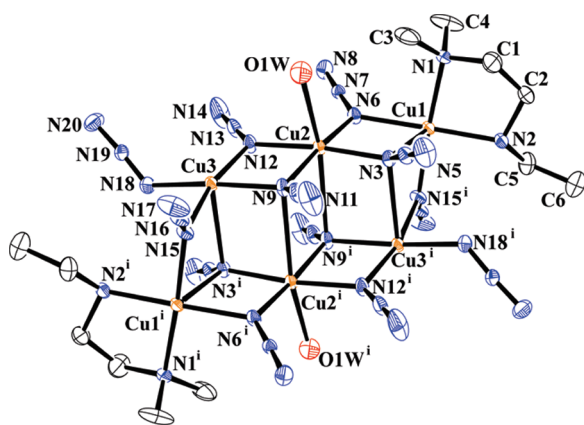


Figure 3. ORTEP view of the basic unit of **2**. Hydrogen atoms have been removed for clarity. Thermal ellipsoids are at the 30% probability level.

distorted octahedral geometries. Cu1 has two nitrogen atoms from the diamine ligand (N1, N2) and two other $\mu_{1,1}$ nitrogen atoms of two azido ligand (N6, N15) in its equatorial plane with the bonds in the range 2.016(2)–2.038(2) Å. The two axial nitrogen atoms are provided by one $\mu_{1,1,1}$ azido [Cu1–N3, 2.427(3) Å] and one $\mu_{1,1,3}$ azido [Cu1–N17^{#9}, 2.576(3) Å] group from an adjacent Cu_6^{II} unit. Cu2 forms its equatorial bonds with two $\mu_{1,1}$ nitrogen atoms [Cu2–N6, 1.983(3) Å; Cu2–N12, 2.028(2) Å] and two $\mu_{1,1,1}$ nitrogen atoms [Cu2–N3, 1.994(2) Å; Cu2–N9, 1.993(3) Å] of four azido groups, whereas the axial bonds are formed by one $\mu_{1,1,1}$ nitrogen atom [Cu2–N9^{#1}, 2.782(3) Å] and another $\mu_{1,3}$ -azido nitrogen atom [Cu2–N20^{#8}, 2.470(3) Å] from an adjacent unit. The equatorial sites of Cu3 are occupied by two $\mu_{1,1}$ nitrogen atoms trans to each other (N12, N15), one $\mu_{1,1,1}$ nitrogen (N9) and one nitrogen from a $\mu_{1,3}$ azido ligand (N18) with the bonds in the range from 1.946(3) to 2.036(3) Å. The axial sites are taken up by one $\mu_{1,1,1}$ nitrogen [Cu3–N3^{#1}, 2.425(3) Å] and one nitrogen atom from a $\mu_{1,1,3}$ azido group [Cu3–N14^{#8}, 2.787(4) Å] from an adjacent unit.

Within the basic Cu^{II}_6 core, the Cu–N($\mu_{1,1}$)–Cu angles are spread within the range 85.68(8)°–108.16(12)°. The adjacent Cu–Cu distances are within the range of 3.1128(6)–3.6134(6) Å. Each Cu^{II}_6 unit is joined with two neighboring such units through double $\mu_{1,3}$ azido bridges and double

$\mu_{1,1,3}$ azido bridges along the a axis and with two other units through double $\mu_{1,1,3}$ azido ligands parallel to the c axis to yield a 2D network (Figure 4b).

Structure Description of $[\text{Cu}_6(\text{N}_3)_{12}(\text{hmpz})_2]_n$ (4**).** Single-crystal X-ray studies reveal that compound **4** crystallizes in a monoclinic space group $P2_1/c$ and is made up of hexanuclear building units (Figure 6a) extended in one dimension. The asymmetric unit contains three Cu^{II} atoms, one homopiperazine ligand (coordinated to Cu1), and six azido groups. The three Cu^{II} atoms within the linear trinuclear asymmetric unit are linked by double end-on azido bridges. The copper atom attached to the chelating ligand and its adjacent metal atom (Cu1 and Cu2) have square pyramidal geometry, while Cu3 has square planar geometry. The four basal nitrogen atoms of Cu1 are provided by the hmpz [Cu1–N1, 1.990(2) Å; Cu1–N2, 1.986(2) Å] and two end-on bridging azido groups [Cu1–N3, 1.996(3) Å; Cu1–N6, 1.999(3) Å] that link to the Cu2 atom, while the apical nitrogen comes from a $\mu_{1,3}$ azido group [Cu1–N20, 2.474(3) Å] that joins it to the Cu3 atom of an adjacent trinuclear unit. All four basal nitrogen atoms (N3, N6, N9, N12) for Cu2 are provided by $\mu_{1,1}$ azido groups (linking it to the adjacent copper atoms), with bonds in the range from 1.966(3) to 1.999(3) Å. The apical position is taken up by a nitrogen atom from a $\mu_{1,1}$ azido group [Cu2–N15^{#10}, 2.488(3) Å] that links to the Cu3 atom of the adjacent unit. The square planar Cu3 atom has three $\mu_{1,1}$ nitrogen atoms (N9, N12, N15) and one nitrogen atom (N18) from a $\mu_{1,3}$ azido bridge, with the bonds in the range from 1.932(3) to 2.035(3) Å. Two adjacent units are thus joined by one end-on (N15–N16–N17) and one end-to-end azido (N18–N19–N20) groups and this structure repeats itself in one dimension along the crystallographic c axis (Figure 6b), owing to the simultaneous operation of the symmetry elements (inversion center at the origin, 2-fold screw axis and the glide plane perpendicular to it).

Structural Correlation of the Four Complexes. To the best of our knowledge, only three Cu^{II}_6 –azido complexes are known in the literature, $\text{Cu}_6(\text{N}_3)_{12}(\text{N-Eten})_2$ (**1A**), $\text{Cu}_6(\text{N}_3)_{12}(\text{N-Ipren})_2$ (**1B**), $\text{Cu}_6(\text{N}_3)_{12}(\text{deen})_2$ (**1C**).¹¹ Complex **1**, along with all these three complexes, share the same 3D structure, with identical connectivity. But **2** and **3** are unique, as in spite of possessing the same Cu^{II}_6

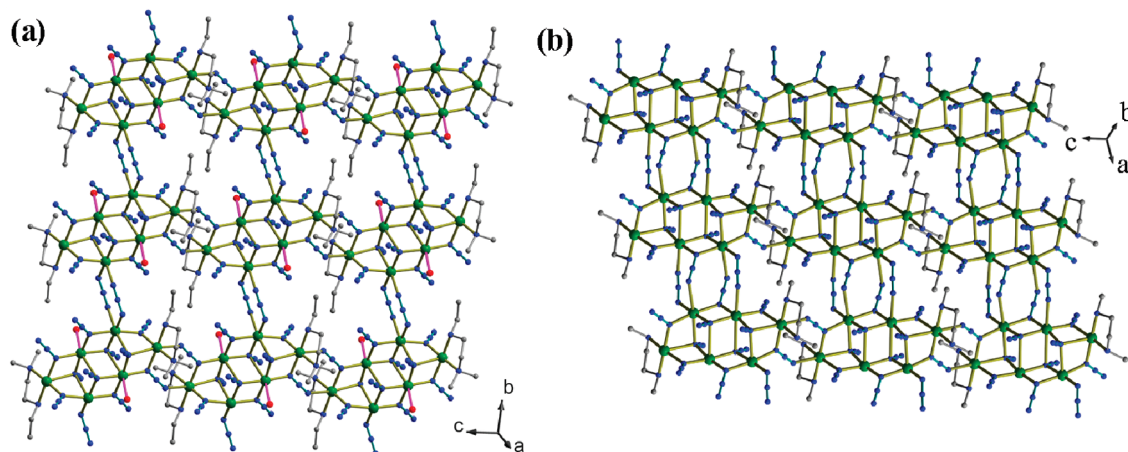


Figure 4. Ball and stick view of the 2D arrangement of the Cu^{II}_6 units (a) for **2** and (b) for **3** illustrating their different connectivities. Color code: copper – green, nitrogen – blue, carbon – gray, oxygen – red. Hydrogen atoms have been removed for clarity.

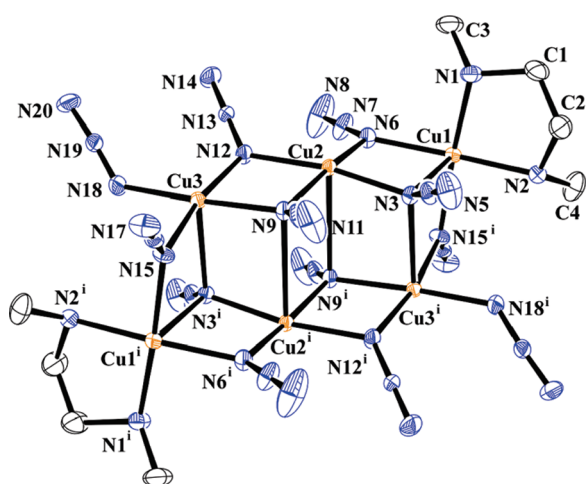


Figure 5. ORTEP view of the basic unit of **3**. Hydrogen atoms have been removed for clarity. Thermal ellipsoids are at the 30% probability level.

building units they are 2D in nature. More interestingly, the two 2D structures differ substantially in the linking patterns between the building units (Figure 4). It is difficult to rationalize these outcomes, based on just the differences in the diamine ligands. But it would seem justified to say that the two coordinated water molecules (to Cu2) block the two copper atoms to participate in the linking of the building units through azido bridges. But for **3**, it is rather surprising to get an overall 2D structure; when we compare the bond parameters within the hexanuclear building unit with **1** (Table 2), the differences are too small to justify the observation. Between **2** and **3**, the differences in the linking patterns can be attributed to the coordinated water molecules in **2**.

When complex **4** is considered in this discussion, we can see that it too has a linear trinuclear crystallographic asymmetric unit in which the adjacent copper atoms are linked by double end-on azido bridges. The difference with the other three complexes seems to be in the linking of these asymmetric units. But a closer look at the distribution of the short equatorial bonds in **1**–**3** of the metal atoms shows that Cu1 links to Cu2 in an axial–equatorial manner through one of the end-on azido bridges, while in **4** the equatorial bonds in the asymmetric units are all in

almost the same plane (Figure 7). For **4**, the diamine is a little bit different sterically; as unlike the other three, there are dimethylene and trimethylene groups situated above and below the chelating plane (N1, N2, Cu1) of the diamine. The steric effects of these alkyl groups may limit the end-on azido bridges close to the chelating plane and thus a very different structure emerges.

Magnetic Behavior

Complex 1. The *dc* magnetic susceptibility measured on a polycrystalline sample of **1** under an applied field of 2000 G is shown in Figure 8 as both χ_M vs *T* and $\chi_M T$ vs *T* plots (where χ_M is the molar magnetic susceptibility per Cu_6^{II} unit). At room temperature (300 K), the $\chi_M T$ value is $2.80 \text{ cm}^3 \text{ K mol}^{-1}$, which is a little higher than expected for six uncoupled Cu^{II} ions ($\chi_M T = 0.375 \text{ cm}^3 \text{ K mol}^{-1}$ for an $S = 1/2$ ion with $g = 2.0$). The $\chi_M T$ value gradually increases upon lowering the temperature and shows a rapid jump below 75 K, to reach a maximum value of $5.90 \text{ cm}^3 \text{ K mol}^{-1}$ at 18 K. Below this temperature, the $\chi_M T$ value decreases sharply (saturation effect) to $2.18 \text{ cm}^3 \text{ K mol}^{-1}$ at 1.8 K. The $1/\chi_M$ vs *T* plots (300–25 K) obey the Curie–Weiss law (Figure S1, Supporting Information) with a positive Weiss constant of $\theta = 24.77 \text{ K}$, which along with the nature of the $\chi_M T$ vs *T* plot indicates a dominant ferromagnetic interaction among the metal ions through azide bridges.

Assuming the exchange pathways in the basic Cu^{II}_6 units (Scheme 2) to be uniform, a reasonable fit is obtained applying the Hamiltonian

$$H = -J(S_1 S_2 + S_2 S_3 + S_3 S_4 + S_4 S_5 + S_5 S_6 + S_6 S_1)$$

and introducing an intercluster zJ' term. Considering the two different exchange parameters, the analysis of the experimental susceptibility values has been performed using the following expression:

$$\chi_M = \chi_M' / \{1 - \chi_M' (2zJ' / Ng^2 \beta^2)\} + \alpha_{(\text{TIP})}$$

$$\chi_M' = (2Ng^2 \beta^2 / KT)[A/B]$$

where $A = 14 + 9 \exp(-5J/kT) + 25 \exp(-3J/kT)$ and $B = 7 + 27 \exp(-5J/kT) + 5 \exp(-6J/kT) + 25 \exp(-3J/kT)$.

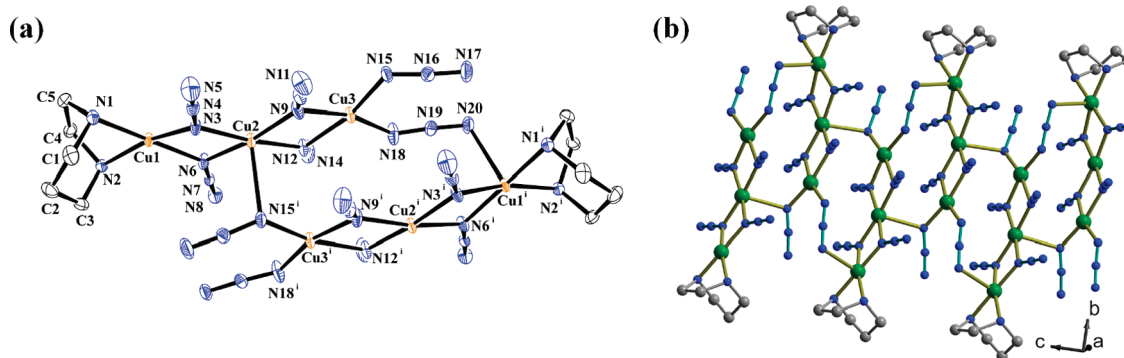


Figure 6. (a) ORTEP view of the basic unit of **4**. Thermal ellipsoids are at 30% probability level. (b) Ball and stick representation of the 1D chain of **4**. Color code: copper – green, nitrogen – blue, carbon – gray. Hydrogen atoms have been removed for clarity.

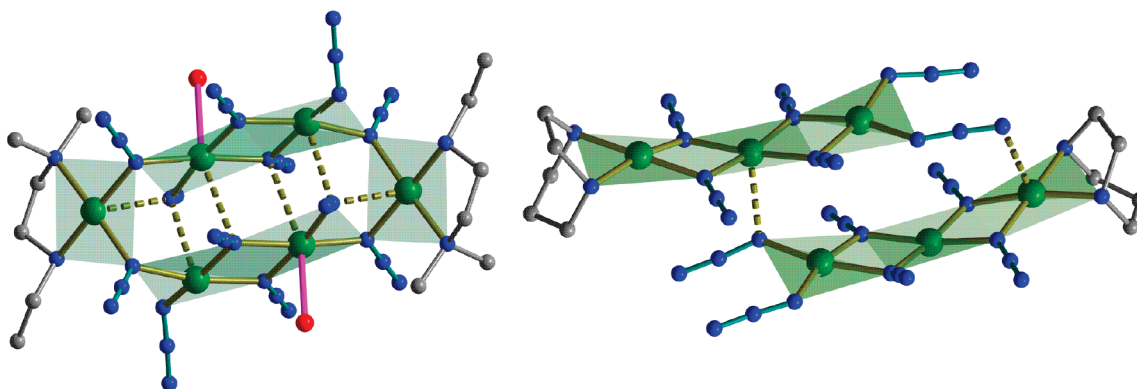


Figure 7. Comparison of the basic structural units of **2** (left, representing **1–3**) and **4** (right). The shaded planes are the equatorial planes of the individual copper atoms. Color code: copper – green, nitrogen – blue, carbon – gray, oxygen – red. Hydrogen atoms have been removed for clarity.

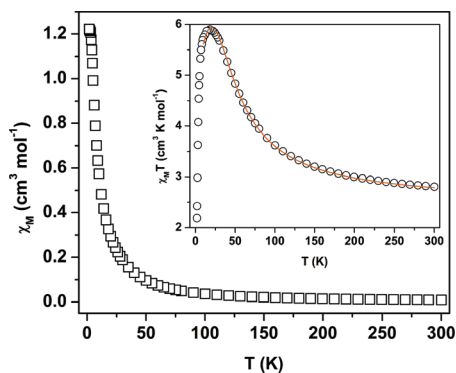


Figure 8. Plots of χ_M vs T and $\chi_M T$ vs T (inset) for complex **1** in the temperature range of 1.8–300 K. The brown solid line indicates the fitting using theoretical model (see text).

The values giving the best fit (8–300 K) are $J = 11.15 \text{ cm}^{-1}$, $zJ' = -0.14 \text{ cm}^{-1}$, $g = 2.08$, and $\alpha_{(\text{TIP})} = 0.0075 \text{ cm}^3 \text{ mol}^{-1}$ ($R = 7.28 \times 10^{-5}$). Out of the three isostructural complexes pointed out earlier **1A** and **1B** shows ferromagnetic behavior with weak intercluster ferromagnetic ordering at lower temperatures, while **1C** was found to behave similar to **1**, with weak intercluster antiferromagnetic interactions.¹¹

Complex 2. Figure 9 shows the temperature dependence of χ_M and $\chi_M T$ values for complex **2** (where χ_M is the molar magnetic susceptibility per Cu_6^{II} unit). The room temperature (300 K) $\chi_M T$ value $2.74 \text{ cm}^3 \text{ K mol}^{-1}$ is again slightly higher than expected for six uncoupled Cu^{II} ions and increases gradually up to $3.98 \text{ cm}^3 \text{ K mol}^{-1}$ upon

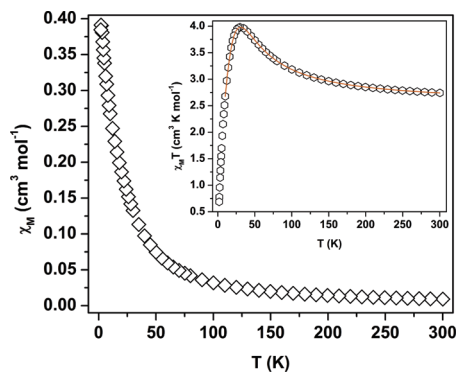
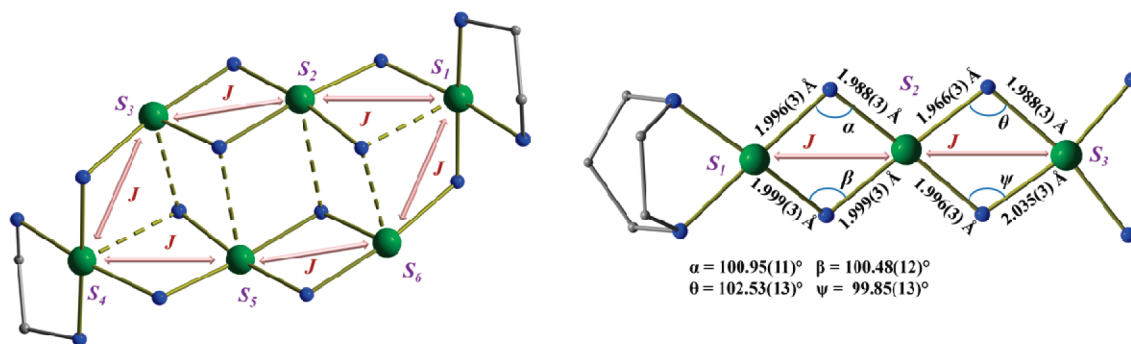


Figure 9. Plots of χ_M vs T and $\chi_M T$ vs T (inset) for complex **2** in the temperature range of 1.8–300 K. The brown solid line indicates the fitting using theoretical model (see text).

lowering the temperature to 30 K. Below this temperature, the $\chi_M T$ value decreases rapidly to $0.68 \text{ cm}^3 \text{ K mol}^{-1}$ at 1.8 K. The $1/\chi_M$ vs T plots (300–25 K) obey the Curie–Weiss law (Figure S1, Supporting Information) with a positive Weiss constant of $\theta = 14.75 \text{ K}$. The nature of the $\chi_M T$ versus T plot and the positive θ suggest a dominant ferromagnetic exchange among the six Cu^{II} ions through azido bridges.

As the Cu_6^{II} building unit of **2** is almost identical to that of **1**, the same model was used to fit the magnetic data. The values giving the best fit (10–300 K) are $J = 8.45 \text{ cm}^{-1}$, $zJ' = -1.29 \text{ cm}^{-1}$, $g = 2.12$, and $\alpha_{(\text{TIP})} = 0.0066 \text{ cm}^3 \text{ mol}^{-1}$ ($R = 1.11 \times 10^{-5}$).

Scheme 2. Schematic Diagrams Representing the Exchange Interaction Models Used for Complex **1–3** (left) and Complex **4** (right)^a

^aThe fragmented bonds are the longer axial bonds.

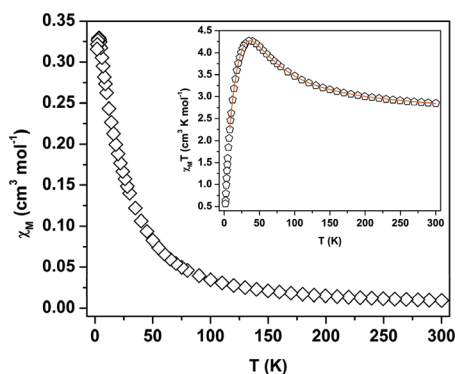


Figure 10. Plots of χ_M vs T and $\chi_M T$ vs T (inset) for complex **3** in the temperature range of 1.8–300 K. The brown solid line indicates the fitting using a theoretical model (see text).

Complex 3. The temperature dependence of magnetic susceptibility of **3** in the form of $\chi_M T$ and χ_M versus T is displayed in Figure 10. At room temperature, the value of $\chi_M T$ is $2.84 \text{ cm}^3 \text{ K mol}^{-1}$, which is slightly above the expected value of $2.25 \text{ cm}^3 \text{ K mol}^{-1}$ expected for six uncoupled Cu^{II} ions. Upon cooling, the $\chi_M T$ value increases slowly and then more rapidly below 75 K to reach the value of $4.27 \text{ cm}^3 \text{ K mol}^{-1}$ at 34 K, and then falls very rapidly to $0.56 \text{ cm}^3 \text{ K mol}^{-1}$ at 1.8 K, indicating the ferromagnetic coupling between the Cu^{II} ions. Accordingly, the $1/\chi_M$ vs T plot (300–25 K) follows the Curie–Weiss law (Figure S1, Supporting Information) with a positive Weiss constant of $\theta = 19.01 \text{ K}$.

The Cu_6^{II} building unit of **3** can be treated similarly to that of **1** and **2**, and thus the same model can be used to fit the magnetic susceptibility data. The values giving the best fit (8–300 K) are $J = 10.96 \text{ cm}^{-1}$, $zJ' = -1.34 \text{ cm}^{-1}$, $g = 2.13$, and $\alpha_{(\text{TIP})} = 0.0052 \text{ cm}^3 \text{ mol}^{-1}$ ($R = 1.34 \times 10^{-5}$).

Complex 4. The magnetic susceptibility data of **4** were measured in the 1.8–300 K temperature range at 2 kOe, and they are shown as $\chi_M T$ and χ_M (where χ_M is the molar magnetic susceptibility per Cu_3^{II} unit) versus T plots (Figure 11). The experimental $\chi_M T$ value of **4** at room temperature is $1.37 \text{ cm}^3 \text{ K mol}^{-1}$, which is somewhat higher than the spin-only value ($1.125 \text{ cm}^3 \text{ K mol}^{-1}$) expected for three magnetically isolated Cu^{II} ions. The $\chi_M T$ value gradually increases upon lowering the temperature to reach a maximum value of $1.76 \text{ cm}^3 \text{ K mol}^{-1}$ at 30 K. Below this temperature, the $\chi_M T$ value decreases sharply to $0.70 \text{ cm}^3 \text{ K mol}^{-1}$ at 1.8 K. The $1/\chi_M$ vs T plot

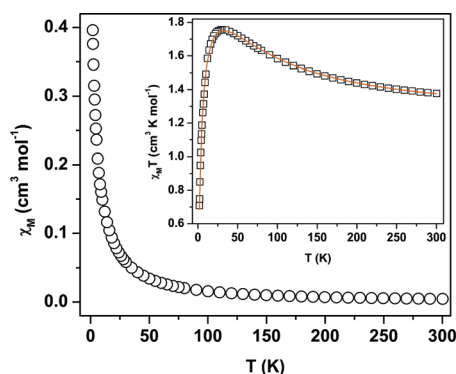


Figure 11. Plots of χ_M vs T and $\chi_M T$ vs T (inset) for complex **4** in the temperature range of 1.8–300 K. The brown solid line indicates the fitting using a theoretical model (see text).

above 30 K is exactly linear following the Curie–Weiss law (Figure S1, Supporting Information) with a positive $\theta = 12.55 \text{ K}$ supporting ferromagnetic interaction between the metal ions through azido bridges.

From the structural point of view, the three copper atoms are bridged by double end-on azido groups in a linear fashion and the bridging angles, and the corresponding bond distances are so similar (Scheme 2) that an isotropic exchange model is very suitable for the analysis of the susceptibility data. A reasonable fit can be obtained for interacting trinuclear units applying the conventional Hamiltonian:

$$H = -J(S_1 S_2 + S_2 S_3)$$

introducing an intertrimer zJ' term. Considering these two different exchange parameters, the analysis of the experimental susceptibility values has been performed using the following expression:

$$\chi_M = \chi_M' / \{1 - \chi_M' (2zJ' / Ng^2 \beta^2)\} + \alpha_{(\text{TIP})}$$

$$\chi_M' = (Ng^2 \beta^2 / 3KT) [A/B]$$

where $A = [15 \exp(3J/2kT) + (3/2) \exp(J/kT) + (3/2)]$ and $B = [4 \exp(3J/2kT) + 2 \exp(J/kT) + 2]$.

The values giving the best fit (1.8–300 K) are $J = 91.24 \text{ cm}^{-1}$, $zJ' = -0.99 \text{ cm}^{-1}$, $g = 2.08$, and $\alpha_{(\text{TIP})} = 0.0017 \text{ cm}^3 \text{ mol}^{-1}$ ($R = 1.25 \times 10^{-5}$).

A literature survey shows that the double end-on azido bridged copper complexes with all the bridging bonds

near 2.0 Å (equatorial bonds) and the Cu–N($\mu_{1,1}$)–Cu angles in the range 100.0–102.0° have the experimental exchange coupling constant J in the range 25–145 cm⁻¹.¹⁸ From Scheme 2, it is evident that bond parameters of **4** fall well within this range (average bond distance \sim 1.99 Å, angle \sim 100.9°) and thus the experimental J value also fits the trend.

Concluding Remarks

The amount of blocking amine in principle should change the structural pattern of azido-metal systems. A strategy to have more coordination sites available around the metal center for a short bridging ligand like azide may bring several metal ions closer and favor the formation of the cluster as a building unit. For this purpose, use of lower equivalents of blocking amine is expected to be fruitful. While in majority of the cases one or two equivalents of blocking amines have been used to generate several azido bridged coordination polymers, we are able to isolate four complicated coordination

polymers (**1–4**) of Cu₆ clusters as repeating units using less than one equivalent of blocking amines. The complexes synthesized are of various dimensionalities, from simple 1D to complicated 3D networks. The effect of coordinated water molecules to block the bridging options through azido linkers also showed how different arrangements of the building blocks can give rise to two very different 2D structures (**2** and **3**). The temperature-dependent magnetic susceptibility measurements showed that all the four complexes are predominantly ferromagnetic with various degrees of intercluster antiferromagnetic interactions. In short this study shows the potential of using various blocking amine ligands in less than one equivalent with respect to the metal in conjunction with azido and other pseudo halides and the formation variety of assemblies with interesting structures and properties.

Acknowledgment. S.M. gratefully acknowledges the Council of Scientific and Industrial Research, New Delhi, India, for the award of a Research Fellowship. Authors also thank the Department of Science and Technology (DST), New Delhi, for financial support. Authors sincerely thank Prof. You Song for the magnetization measurements of **1**.

Supporting Information Available: X-ray crystallographic data in CIF format, Curie–Weiss fitting of the $1/\chi_M$ vs T data, and M vs H plots of **1–4**. This material is available free of charge via the Internet at <http://pubs.acs.org>.

(18) (a) Aebersold, M. A.; Gillon, B.; Plantevin, O.; Pardi, L.; Kahn, O.; Bergerat, P.; Seggern, I. V.; Tucek, F.; Öhrström, L.; Grand, A.; Lelièvre-Berna, E. *J. Am. Chem. Soc.* **1998**, *120*, 5238. (b) Sun, W.-W.; Qian, X.-B.; Tian, C.-Y.; Gao, E.-Q. *Inorg. Chim. Acta* **2009**, *362*, 2744. (c) Sikorav, S.; Bkouche-Waksman, I.; Kahn, O. *Inorg. Chem.* **1984**, *23*, 490. (d) Youngme, S.; Chotkhun, T.; Leelasubcharoen, S.; Chaichit, N.; Pakawatchai, C.; van Albada, G. A.; Reedijk, J. *Polyhedron* **2007**, *26*, 725. (e) Woodward, J. D.; Backov, R. V.; Abboud, K. A.; Dai, D.; Koo, H.-J.; Whangbo, M.-H.; Meisel, M. W.; Talham, D. R. *Inorg. Chem.* **2005**, *44*, 638.